

Latitudinal Distribution of the Parameters of Internal Gravity Waves in the Atmosphere Derived from Amplitude Fluctuations of Radio Occultation Signals

V. Kan^{a, *}, M. E. Gorbunov^{a, b}, O. V. Fedorova^a, and V. F. Sofieva^c

^a*Obukhov Institute of Atmospheric Physics, Russian Academy of Sciences, Moscow, 119017 Russia*

^b*Hydrometeorological Research Center of the Russian Federation, Moscow, 123242 Russia*

^c*Finnish Meteorological Institute, P.O. BOX 503, Helsinki, FI-00101 Finland*

**e-mail: valerykan@list.ru*

Received April 16, 2020; revised June 15, 2020; accepted August 5, 2020

Abstract—The method of reconstructing the global distribution of statistical parameters of internal gravity waves (IGWs) in the atmosphere has been tested using the data of amplitude fluctuation measurements of a radio signal in satellite radio occultation (RO) observations. In our previous work, for the chosen model of the spatial IGW spectrum, its relationship with the spectra of amplitude fluctuations was obtained, an algorithm for reconstructing the model parameters was developed, and the reconstruction errors were estimated. The reconstructed parameters of the vertical IGW spectrum are the external scale, which separates the unsaturated large-scale waves from saturated small-scale waves, and the structural characteristic, which determines the spectral amplitude of saturated waves. These parameters are used to calculate the variance of temperature fluctuations and the potential energy of the waves. This article presents the altitude–latitude distribution of IGW parameters in the stratosphere according to the measurements of the COSMIC experiment in 2011. The characteristic features of these distributions are noted, and the results are compared with the data of other measurements.

Keywords: radio occultation sounding of the atmosphere, signal amplitude fluctuations, reconstruction of internal gravity wave parameters, global distribution of wave parameters

DOI: 10.1134/S0001433820060055

INTRODUCTION

This paper presents the results of reconstructing the altitude–latitudinal distribution of internal gravity wave (IGW) parameters from the data of COSMIC (Constellation Observing System for Meteorology Ionosphere and Climate) satellite measurements carried out in January–February and June–July 2011. The technique for reconstructing the IGW parameters [1], is based on the relations between the IGW spectra and the amplitude fluctuations of radio occultation signals. For IGW parametrization, the model of the three-dimensional spectrum of anisotropic atmospheric irregularities [2–5] developed by A.S. Gurvich has been chosen, which is a generalization of the one-dimensional “universal” vertical spectrum of temperature fluctuations generated by an ensemble of saturated internal waves [6–8]. The main parameters of the three-dimensional spectrum model, which can be reconstructed from fluctuations of radio occultation signals, are the external vertical scale L_W and the structural characteristic C_W^2 . The L_W scale separates the unsaturated (large-scale) and saturated (small-scale)

intervals of the wave spectrum, and the main wave power is concentrated at scales close to L_W . The C_W^2 structural characteristic is the only parameter that determines the spectral density of waves in the saturation mode [1, 6–10]. The values of these parameters in our work are selected so that the theoretical spectra are as close as possible to the experimental ones. The technique is similar to that for reconstructing the IGW parameters and turbulence from optical satellite observations of stellar scintillation [2–5]; the differences are due to the significant difference in wavelengths. The relevance of research is determined by the fact that IGWs are the main source of mesoscale fluctuations of wind and temperature with vertical scales from several kilometers to hundreds of meters and with periods from several minutes to 10 h. They play a key role in energy exchange and global atmospheric circulation, temperature-field formation, turbulence generation, and mixing [8, 10].

To test the technique developed in [1], we reconstruct the altitude–latitude distribution of IGW parameters in the stratosphere. This article is structured as fol-

lows. The section Parameters Being Reconstructed discusses the question of what wave parameters can be reconstructed from measurements of fluctuations of the radio occultation signal amplitude. In the section Profiles of Latitude-Averaged Parameters, for two seasons, the reconstructed altitude profiles of the external scale values averaged over latitude bands, structural characteristics, and RMS temperature fluctuations, their discussion, and comparative analysis with the data of other works are presented. The section Latitudinal Distribution of Potential Energy contains the reconstructed latitudinal distributions of potential energy of IGWs for two altitude intervals: 16–24 and 24–28 km, a comparison with other works, and discussion. The Conclusions summarize the main results of the work.

1. PARAMETERS BEING RECONSTRUCTED

The procedure for analyzing the radio-signal-amplitude measurement data and the recovery technique are discussed in detail in [1]. The adopted three- and one-dimensional models of internal waves (1) and (2) in [1] are determined by external scale L_w , structural characteristic C_w^2 , anisotropy coefficient η , internal scale l_w , and the exponent of the spectrum μ in the power-law section [2–5]. We adopt the spectrum slope $-\mu$ equal to -5 for three-dimensional spectrum and $-\mu + 2 = -3$ for the one-dimensional vertical spectrum in accordance with the model of the “universal” spectrum of saturated internal waves [6–8]. The agreement in slope $-\mu$ of the spectra of amplitude fluctuations of the radio signal and the “universal” spectrum of saturated waves was demonstrated in [11]. The main scale of the amplitude fluctuations of the radio signal is the Fresnel scale ρ_F , which is determined by the geometry of observations and equals 1.0–1.5 km in the stratosphere for GPS wavelengths (19–24 cm). The internal scale l_w —the scale of wave breaking and their transformation into turbulence—in the stratosphere ranges from ten to several tens of meters [3, 4, 6, 12]. Due to the rapid diffractive decay of the amplitude spectra and the influence of noise, scales as small as l_w have practically no effect on the energy characteristics of the waves and radio signal fluctuations. The statistical problem of wave propagation in a radio occultation experiment is considered for a random field of fluctuations of the refractive index locally uniform in a spherical layer of the atmosphere. The main scales of the problem are Fresnel scale ρ_F and outer scale L_w ; the latter in the stratosphere is several kilometers [1, 2, 6, 7, 13, 14]. For IGWs with vertical scales on the order of a kilometer, anisotropy η exceeds the critical value $\eta_{cr} \approx 30$ and the fluctuations of the radio signal saturate, reaching the limit of spherically layered inhomogeneities [1, 2, 11, 14–16], and are independent of η . Thus, only two parameters are subject to recovery—external scale L_w and the structural characteristic of C_w^2 .

These parameters have been reconstructed in the altitude range of 16–28 km in the polar zones and 22–28 km in the tropics. To this end, 20 000 measurement sessions were used in both seasons: January–February and June–July 2011. The reconstructed parameters were used to calculate the integral energy characteristics—the variance of temperature fluctuations $\sigma_{\delta T}^2$ and the specific potential energy of waves E_p [8–10, 17]:

$$\sigma_{\delta T}^2 = \frac{1}{3\pi} \bar{T}^2 C_w^2 L_w^2, \quad (1)$$

$$E_p = \frac{g^2}{2\bar{T}^2 \omega_{B.V.}^2} \sigma_{\delta T}^2. \quad (2)$$

Where \bar{T} is the profile of average (regular) temperature, $\omega_{B.V.}$ is the Brunt–Väisälä frequency, and g is the acceleration of gravity. Here, the variance of temperature fluctuations $\sigma_{\delta T}^2$ is equal to the integral of the spectrum of temperature fluctuations over the entire range of vertical wave numbers [1].

The external scale in our models, as in [6, 7], determines the plateau of the spectrum in the large-scale region corresponding to unsaturated waves. The form of the spectrum in the transition range between the regions of unsaturated and saturated waves and the L_w definition depend on the specific parameterization of the spectrum. The dominant scale is often used, defined as the position of maximum of the product of the vertical IGW spectrum by the wave number [13, 17–20]. In our model, the ratio of the dominant to the external scale is 1.4 [1]. Despite the importance of the external scale, which determines the intensity of temperature fluctuations and the potential energy of waves, it is perhaps the least studied parameter [6, 7]. In most papers that study the global distribution of IGW parameters, either a saturated wave regime is investigated or integral characteristics are determined: the variance of temperature or velocity fluctuations and the specific potential and kinetic energies, in which both parameters, C_w^2 and L_w , are inseparably included [9, 21–23]. The most natural estimate of L_w is the scale of the spectrum slope change during the transition from the saturated to the unsaturated wave mode. Typical L_w values in the stratosphere are several kilometers [6, 7], and they are comparable not only with the scale of variations in the regular profile, but also with the lengths of the realizations. Therefore, when interpreting the data, difficulties arise associated with both the separation of the regular and fluctuation profiles in the largest scale region [20, 23–25] and with the statistical instability of spectral estimates in this region. Each measurement method, or “observation filter” [26], has its own selective sensitivity to a certain range of scales of the studied waves. The resolution of the GPS temperature profiles reconstructed in the geometric optical approximation is 1.5–2 km in the stratosphere [21, 27]. An analysis of the observa-

tional filter for temperature fluctuations based on radio occultation measurements [21] shows that the main interval of the scales of representative measurements, or the “main interval” in the stratosphere, extends from about 2 to 5 km. On such a small scale interval, it is not easy to detect both the power-law section with a slope of -3 and the transition to a plateau associated with the outer scale. According to [21], such a transition in the large-scale spectral region near 3–5 km is associated with the filtering procedure rather than with the influence of the external scale. The use of methods based on wave optics can significantly improve the vertical resolution [28, 29].

Another factor that significantly affects the results, changing the potential energy estimates up to several times, is the method of separating the mean and fluctuation temperature profiles [20, 25]. In the term *observational filter*, we will include the difference not only in the measurement methods [26], but also in the methods of analyzing temperature profiles [20, 25]. Unlike processing radio occultation data in the geometric optics approximation, spectra obtained from radiosonde temperature profiles reach much smaller scales of 100–200 m [13, 17, 18, 30]. This makes it possible to better identify both the transition region and the region of saturated waves.

In our calculations, to eliminate the effect of quadratic detrending, used to determine the average profile in individual measurements, we use the spectra of amplitude fluctuations, starting from the scale $\Delta z/3$, where $\Delta z = 8$ km is the length of the selected fragments of realizations. Model calculations show that the effect of quadratic detrending is limited to the first two frequencies. The outer scale manifests itself in the form of a spectrum of amplitude fluctuations up to $L_w \approx 5\text{--}7$ km [1]. Since our method is based on the diffraction theory of fluctuations, the resolution is limited not by the Fresnel scale, but by the measurement and ionospheric noises, and is several hundred meters [11].

At this stage, to test the technique, the altitude–latitudinal distribution of IGW parameters in the latitude bands of $0^\circ\text{--}20^\circ$, $20^\circ\text{--}40^\circ$, $40^\circ\text{--}60^\circ$, and $60^\circ\text{--}90^\circ$ in the Northern and Southern hemispheres was studied according to data of winter and summer 2011 measurements. The upper limit of the altitude range was 32 km, and the lower one was 1 km above the upper limit of the tropopause in the corresponding zone. The spectra of relative amplitude fluctuations were calculated for regions of realizations Δz with a step of 2 km.

2. PROFILES OF LATITUDE-AVERAGED PARAMETERS

Figure 1 shows the altitude profiles of values of external scale L_w averaged over latitudinal bands for the Northern (upper panels (a) and (b)) and Southern (lower panels (c) and (d)) hemispheres. Left panels (a)

and (c) correspond to local winter in the Northern and Southern hemispheres, and right panels (b) and (d) correspond to the local summer in these hemispheres.

The outer scale L_w varies from 2 to 4 km. Tropical latitudes are characterized by the highest L_w values. While in the circumpolar regions the outer scale tends to increase with height, in the tropics the opposite tendency is observed, and the L_w profiles converge at the altitude of 28 km. In the Northern Hemisphere, the winter–summer asymmetry of the profiles is less pronounced than in the Southern Hemisphere. The L_w values can be underestimated due to (1) inaccuracies of spectral estimates on the largest scales, which leads to a limitation of about 5 km scale [1, 12] and (2) the rejection of spectra with ionospheric outliers in the large-scale region [1].

Experimental data on the external scale are scarce and contradictory. This is explained not only by the natural variability of wave sources, wind profiles, and temperature stratification, but also by different observational filters. The traditional method for determining the mean profile by filtering individual profiles in the selected altitude interval, or vertical detrending [20], is widely used in probe [13, 17, 18, 30] and radio occultation measurements [9, 21, 24, 31–33]. The emergence of a large number of receiving satellites providing a dense network of radio occultation soundings made it possible to apply the averaging temperature profiles in given coordinate-time cells, followed by horizontal detrending–filtering of the lowest horizontal modes [19, 22, 34, 35]. In [20, 23], both methods are tested, and in [9, 19, 20, 24, 25, 35] they are analyzed. With vertical detrending, estimates of the external or dominant scale are usually lower than with horizontal detrending [25].

Work [7] is one of the first to consider a model of the altitude dependence of the external waves scale based on experimental data. The outer scale in [7] increases with height, from the values of about 1 km in the troposphere, to 5 km in the stratosphere, and 20 km in the mesosphere; its strong spatiotemporal variability is noticed. According to [36], in the stratosphere for heights below 30 km, the dominant scale values are in the range of 5–10 km by radar and 3–5 km by radiosonde measurements. The dominant scale of about 2 km in the stratosphere was estimated from probe measurements [13]. The dominant scale estimates [18] in the lower stratosphere from the temperature spectra obtained by radiosonde in Illinois, United States (41° N), are 2.5–3.0 km; however, the filtering procedure may affect the shape of the spectrum in the large-scale region. According to [17], the dominant scale values averaged over 5 years at altitudes of 18–25 km decrease from 3 km by 10° N to 2 km by 70° N. The latitudinal contrast is more pronounced for the summer season as compared to the winter one. Similar latitudinal distributions of the dominant scale, obtained from the temperature spectra reconstructed from radio occultation

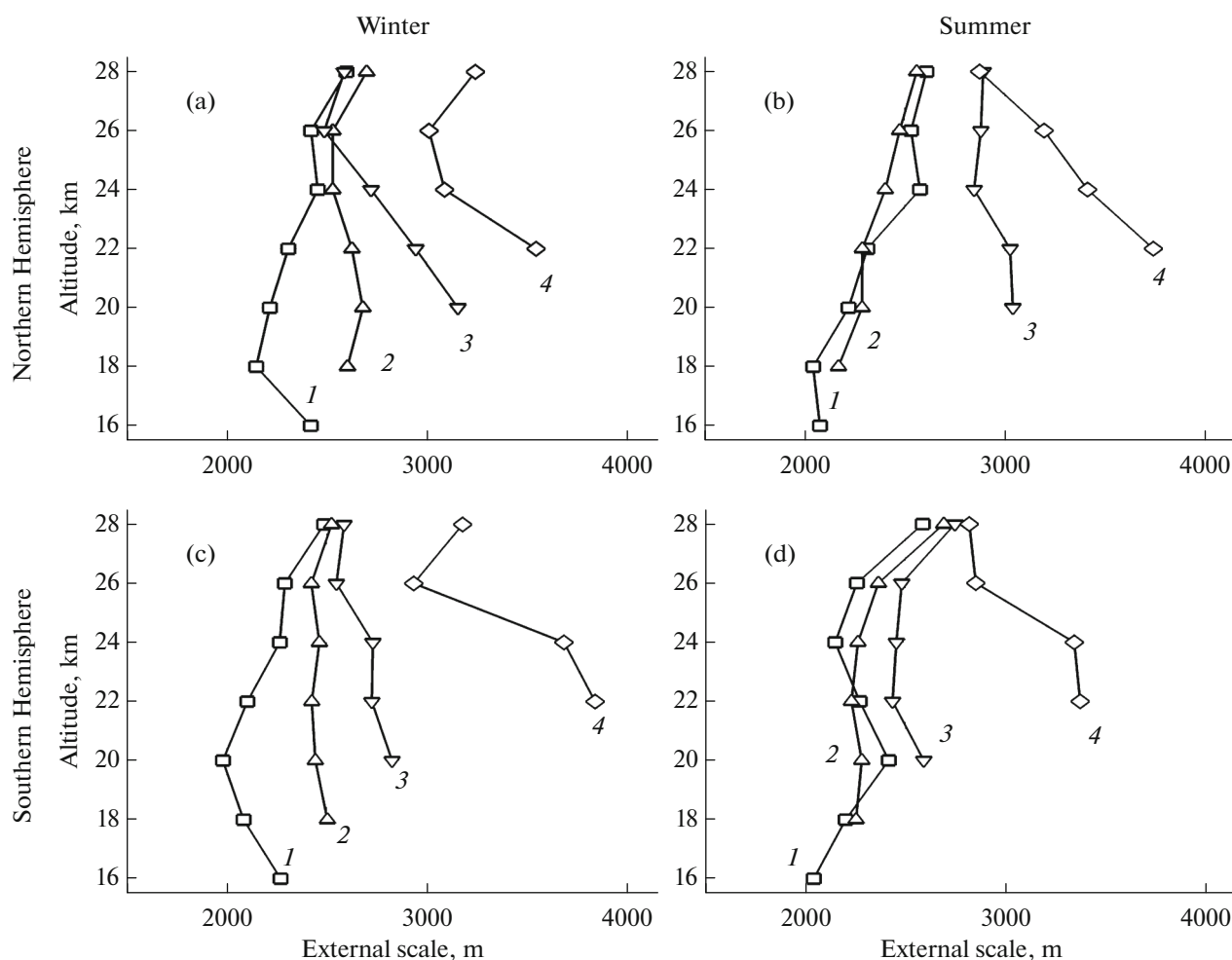


Fig. 1. External scale profiles: (a) Northern Hemisphere, January–February; (b) Northern hemisphere, June–July; (c) Southern Hemisphere, June–July; and (d) Southern Hemisphere, January–February. The numbers on the curves correspond to the latitude bands: (1) 60° – 90° , (2) 40° – 60° , (3) 20° – 40° , and (4) 0° – 20° for the Northern (a, b) and Southern (c, d) hemispheres.

data, are given in [31]: at altitudes of 20–30 km, the dominant scale decreases from 5 km and in the tropics to 3 km in the middle latitudes. The attempts of the authors of [31] to determine the spectrum of temperature fluctuations in the diffraction region by simply decreasing the scale of smoothing of the eikonal data were, as shown in [37], erroneous, but this criticism applies only to the small-scale spectral region. In [38], a method was developed for determining the IGW parameters from the amplitude of temperature fluctuations in the dominant wave; in the given examples of radio occultation measurements [38], the dominant wavelength in the stratosphere at mid-latitudes was 2.0–3.5 km. In [12], the latitudinal distribution of the external scale of IGW at heights of 30–40 km is presented, which was reconstructed from measurements of stellar scintillations with fast photometers onboard the GOMOS/ENVISAT satellite. At heights of 30–34 km, adjacent to the upper boundary of the heights in our measurements, the external scale values decrease from about 3 km in the tropics to 1–2 km in the circumpolar

regions, while at these heights there is no significant change in the latitudinal contrast depending on season. Our values of the external scale shown in Fig. 1 agree with the results [7, 12, 13, 17, 18, 31, 36, 38]. It should be noted that horizontal detrending when processing radio occultation measurements leads to an estimate of the dominant scale, which increases from about 5 km in the tropics to 7–8 km in the circumpolar regions [19] and from 7–8 km in the tropics to 9–10 km in the circumpolar zone [20]. The difference in estimates obtained by different detrending methods and the need to unify data-processing methods are considered in [25].

Figure 2 shows the profiles of the latitude-averaged values of the C_w^2 structural characteristic. Like Fig. 1, the left panels show the profiles for the local winter in the Northern (a) and Southern (c) hemispheres, and, in the right panels, for the local summer in the Northern (b) and Southern (d) hemispheres. The structural characteristic is the only parameter of the saturated wave spectrum. We notice the strong scatter of data

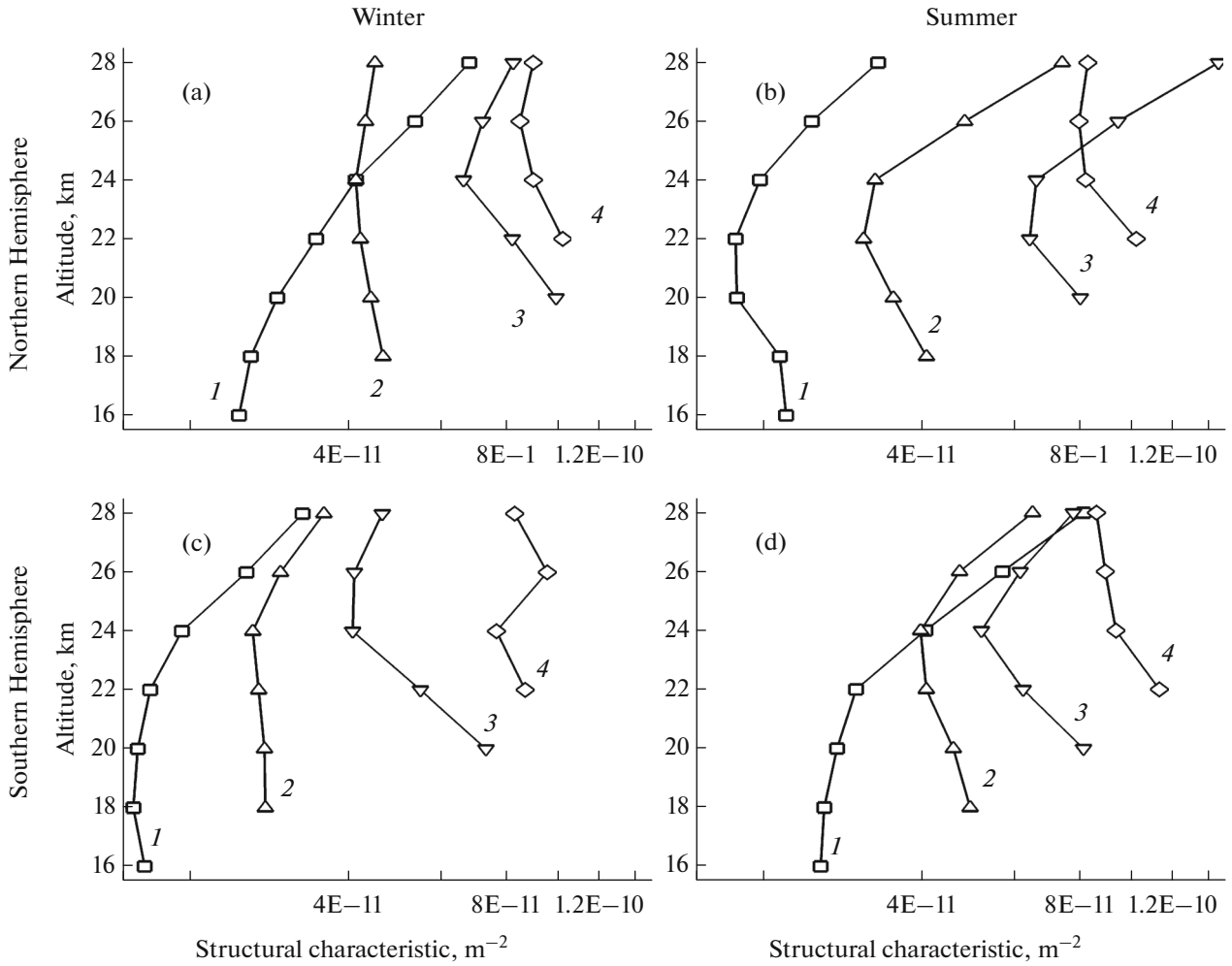


Fig. 2. Profiles of structural characteristic. Designations are the same as in Fig. 1.

both in height and latitude: from $1.5 \times 10^{-11} \text{ m}^{-2}$ to $1.5 \times 10^{-10} \text{ m}^{-2}$. Just as for the outer scale, there is a pronounced increase in values C_W^2 from polar latitudes to tropics, especially at altitudes of 16–22 km. Closer to the upper boundary, the profiles generally converge and the scatter decreases (except for the subtropical profile in panel (b)). In the middle and high latitudes, the C_W^2 values generally slightly increase with altitude, with a small local minimum at 22–24 km. The regular seasonal dependence in the behavior of C_W^2 profiles is not noticeable, perhaps against the background of strong variability of C_W^2 .

The C_W^2 relationship with the spectrum of temperature fluctuations for saturated waves is expressed by the formula (2) in [1]:

$$V_{\delta T/\bar{T}}(\kappa_{z,r}) = \frac{4\pi}{3} C_W^2 \kappa_{z,r}^{-3}, \quad L_W \gg 2\pi/\kappa_{z,r} \gg l_W. \quad (3)$$

For a quantitative comparison of experimental spectra with the model of the “universal” spectrum of

saturated waves [6–8], the wavelengths $\lambda_{z,r} = 2\pi/\kappa_{z,r}$ are usually chosen in the range from several hundred meters to a kilometer [13, 18]. The temperature fluctuation profiles reconstructed from radio occultation observations in the geometric optics approximation do not have the required spatial resolution; therefore, we will compare the C_W^2 profiles we reconstructed with the temperature spectra obtained mainly in radiosonde measurements.

Long-term observations [18] indicate a strong variability of the spectra of saturated waves in individual measurements. The spectral amplitudes given in [18] at the wavelength $\lambda_{z,r} = 0.4 \text{ km}$ show that the values of the structural characteristic C_W^2 at middle latitudes changed tenfold: from $0.4 \times 10^{-11} \text{ m}^{-2}$ to $4.0 \times 10^{-11} \text{ m}^{-2}$, whereas the variability of $\omega_{B.V.}^4$ in these measurements was only 2.5; recall that these parameters are related by linear relation (4) in [1]. In our data, as is shown in Fig. 2a, profiles 2 and 3, the C_W^2 values at midlatitudes were $(3.8\text{--}8.0) \times 10^{-11} \text{ m}^{-2}$. Measurements [13], car-

ried out for 3 years in the subtropics, show that, at altitudes of 18–25 km, the seasonally averaged temperature spectra with wavelengths less than 0.5 km agree satisfactorily with the universal model of saturated waves. However, in the larger scale region of 0.5–1.5 km, noticeable seasonal differences are observed in both the slopes and the values of the spectra. The winter spectra calculated in this range of scales are 1.5–2.0 higher than the model values, and the summer ones are about 2 times lower than the model ones. In [13], these differences are explained by the fact that, in summer, the saturated waves regime shifts towards shorter waves. The data presented in Table 1 [13] make it possible to calculate the seasonally averaged values of the structural characteristic of C_w^2 using the relationship (4) in [1] between C_w^2 and the parameters of model of the universal wave spectrum. The winter C_w^2 values obtained from these data were approximately $1.9 \times 10^{-10} \text{ m}^{-2}$ and the summer ones were $4.5 \times 10^{-11} \text{ m}^{-2}$, which is consistent with our results in the subtropics, except for seasonal differences. In [39], the seasonally averaged spectra of temperature fluctuations at altitudes of 15–25 km, obtained in Antarctica, are given. The maximum values of the structural characteristic $C_w^2 \approx 2.0 \times 10^{-11} \text{ m}^{-2}$ were observed in November, and the minimum values $C_w^2 \approx 0.6 \times 10^{-11} \text{ m}^{-2}$ in February. As in the previous cases, these values are consistent with our polar data in Fig. 2 (curves 1), except for seasonal differences. In [31], the spectrum of temperature fluctuations in the stratosphere over Indonesia is given. The C_w^2 value calculated from the spectral amplitude at $\lambda_{z,r} = 0.5 \text{ km}$ is about $4.0 \times 10^{-11} \text{ m}^{-2}$, which is approximately 2 times lower than our values in the tropics.

In [12], the latitudinal distribution of the structural characteristic at heights of 30–50 km, reconstructed from satellite observations of stellar scintillations, is presented. There is a significant increase in C_w^2 in winter at high latitudes, especially in the Southern Hemisphere: at altitudes close to 30 km, the C_w^2 values in local winter reached $1.0 \times 10^{-10} \text{ m}^{-2}$, and in summer they were about $2.0 \times 10^{-11} \text{ m}^{-2}$. These values are within the range of our data, but they are characterized by increased winter activity at high latitudes. The authors [12] also note a strong variability of the structural characteristic: the latitudinal estimates of C_w^2 at the same altitude could differ by a factor of 10, while the values of $\omega_{B.V.}^4$ differed by no more than 1.6 times.

Figure 3 shows the height profiles of the root mean square deviations (RMSs) of temperature $\sigma_{\delta T}$, calculated according to (1). The values $\sigma_{\delta T}^2$ and E_p are used as a measure of the activity of internal waves. The variance $\sigma_{\delta T}$ in our method is equal to the integral of the

vertical temperature spectrum over the entire range of scales [1]. This should be taken into account when comparing with other works using other observational filters [25, 26]. It follows from (1) and (2) that the temperature variance and potential energy are determined by the wave spectrum in a narrow interval near the outer scale [7–9, 13, 17].

Similar to the outer scale profile and structural characteristics, the profiles of $\sigma_{\delta T}$ also show a strong latitudinal dependence: from 0.6 K in the polar regions to 2.5 K at the equator. This difference is most noticeable at the lower boundaries of the height range, and decreases with height. Large values $\sigma_{\delta T}$ near the lower boundary of the heights in the tropics and subtropics may be partially due to the influence of the tropopause, the altitude range of which is not clearly defined. In polar and middle latitudes, $\sigma_{\delta T}$ generally increase, but all profiles have a small local minimum at altitudes of 22–26 km.

Radiosonde observations of IGW in the tropics [41] indicated that, at altitudes of 20–30 km, values $\sigma_{\delta T}$ vary from 0.5 K to 1.5 K. These values are approximately two times lower than those shown in Fig. 3 of equatorial values. The variance of temperature fluctuations from radiosonde observations in the subtropics [13] was calculated for saturated waves in a narrow range of scales from 0.15 to 0.9 km in order to improve the vertical resolution. Profiles $\sigma_{\delta T}$ for heights of 20–30 km decrease with height, and the winter values slightly exceed the summer ones. However, values $\sigma_{\delta T}$ from 0.15 to 0.3 K are significantly underestimated due to the neglect of large-scale waves. Radiosonde observations of temperature fluctuations with vertical scales up to 4 km in the polar region [42] showed that $\sigma_{\delta T}$ in the stratosphere varies from 0.5 to 1.3 K. This agrees with the polar profiles shown in Fig. 3.

In [9], values $\sigma_{\delta T}^2$ for the equatorial zone and middle latitudes for different seasons are given according to the GPS/MET (GPS Meteorology) experiment. A filter with a scale of 2–10 km was used to allocate fluctuations. Near the equator, at altitudes of 20–30 km, the RMS of temperature $\sigma_{\delta T}$ were 1.6–1.8 K; at mid latitudes they were 1.0–1.2 K and, with some excess in May to August in the Southern Hemisphere, up to 1.45 K. Equatorial data [9] are slightly lower than ours (curve 4 in Fig. 3), and the mid-latitude data are consistent with curve 3 in Fig. 3. In [9], the value of $\sigma_{\delta T}$ is probably underestimated due to the small-scale cutoff of the observational filter at 2 km, associated with the use of the geometric optics approximation in the processing of radio occultation data. The seasonal-latitude distribution of temperature variance from radio occultation data is given in [31]. For comparison with our results, we used the data of Table 2 from [31] for heights of 20–30 km, obtained by filtering temperature fluctuations in the range of scales of 2.5–10 km. In the equatorial zone, the RMSs of temperature $\sigma_{\delta T}$

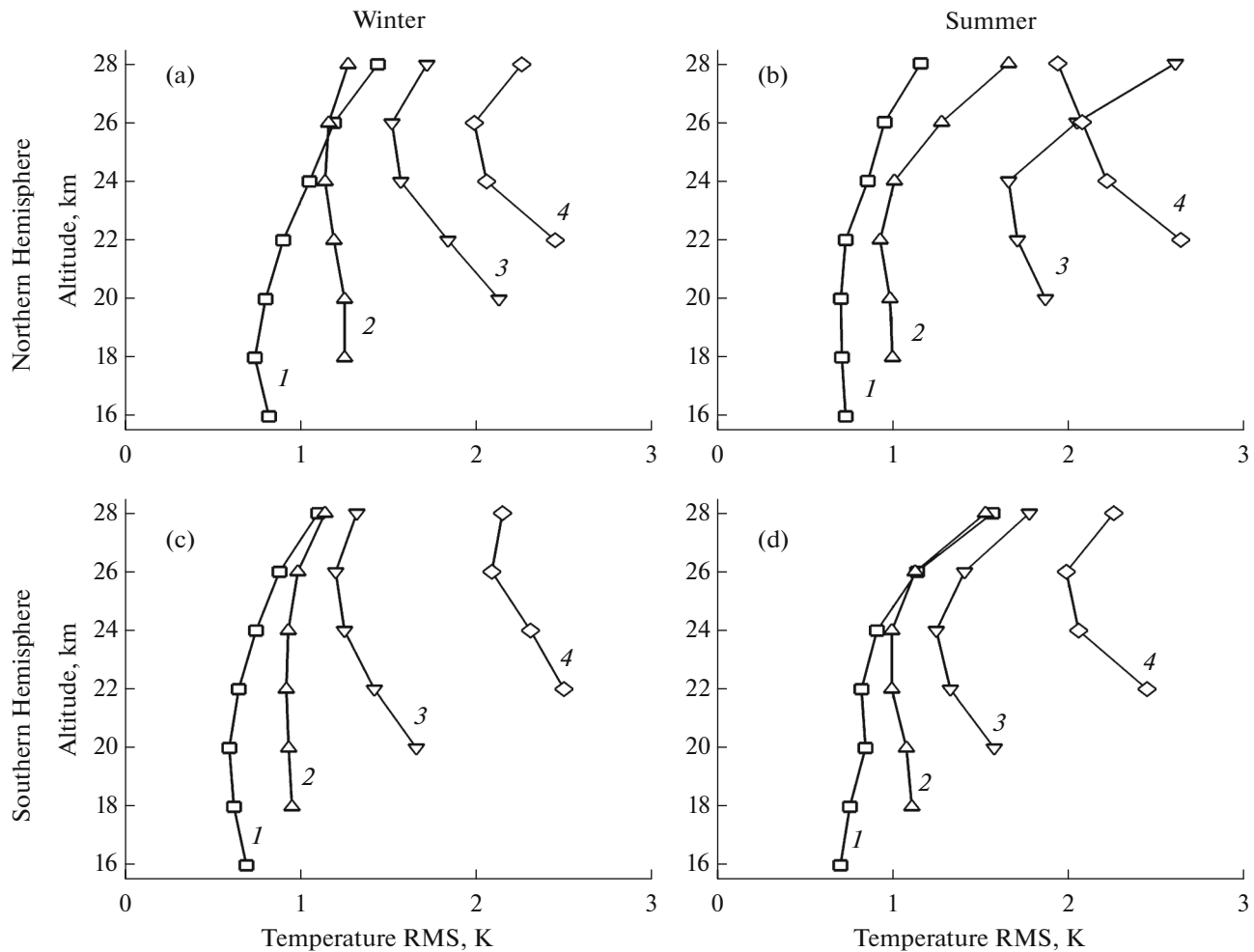


Fig. 3. Profiles of temperature fluctuations. Designations are the same as in Fig. 1.

were of 2.0–2.3 K, in the subtropics, 1.3–1.7 K and 1.1–1.5 K, and in the middle latitudes with an increase in $\sigma_{\delta T}$ to 1.7 K in the Southern Hemisphere in June. These data are consistent with the $\sigma_{\delta T}$ profiles in Fig. 3. In [40], the latitudinal distribution of temperature variance in the stratosphere, averaged over long-term radio occultation measurements, is given. Like in [9], a filter with an upper limit of 10 km was used to separate temperature fluctuations. An increase in $\sigma_{\delta T}$ is noted in the tropics–subtropics, amounting to more than 2 K in the 5-km layer above the tropopause. In middle latitudes, the $\sigma_{\delta T}$ were 1.0–1.5 K and, in the polar regions, 0.7–1.0 K. These data also agree with our results, shown in Fig. 3.

3. LATITUDINAL DISTRIBUTION OF POTENTIAL ENERGY

The most important characteristic of the activity of internal waves is their specific energy (spectral or integral). In radiosonde measurements, both energy components are determined: kinetic energy in terms of the

power of pulsations of the horizontal velocity component and potential energy in terms of the power of temperature fluctuations. In the radio occultation monitoring of IGW, potential energy is used for detecting wave activity [8–10, 17], taking into account the polarization relations between the kinetic and potential energies: in the linear theory, their ratio is equal to the modulus of the exponent of the temporal spectrum of temperature fluctuations [9, 10].

We discuss first the effect of the observational filter on the estimates of potential energy E_p . For our model of the vertical spectrum (2) in [1] and an ideal rectangular filter, the rejection of large-scale waves with $\lambda_z \geq 2L_W$ can lead to an underestimation of E_p by a factor of 2.5. Thus, neglecting scales larger than 5 km can give significantly underestimated E_p , especially in the tropics. Rejecting small-scale waves with $\lambda_z \leq L_W$ can lead to an underestimation of E_p by 20%. In radio occultation temperature profiles, the lower boundary of the observational filter in the stratosphere is about 2 km, which, as follows from Fig. 1, may lead to an underestimation

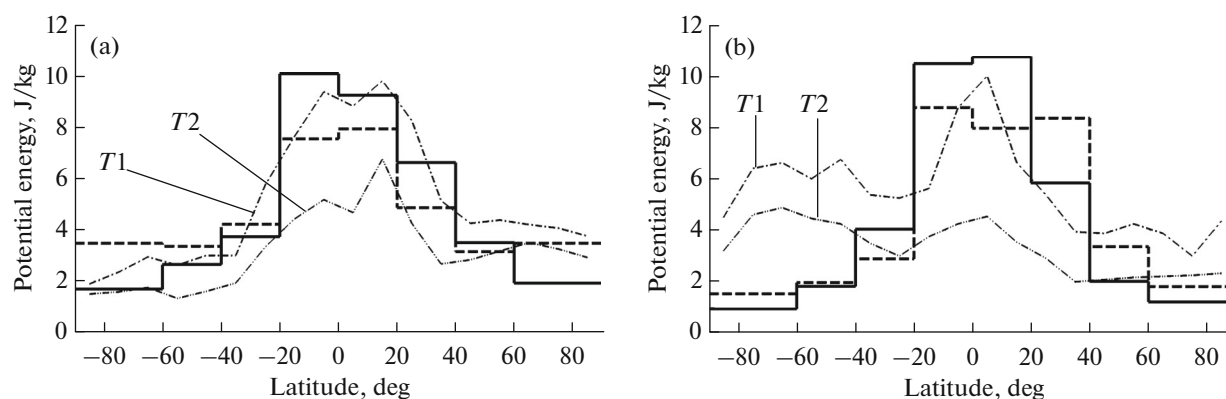


Fig. 4. Latitudinal distribution of the specific potential energy of internal waves at altitudes of 16–24 km (solid lines) and 24–28 km (dashed lines): (a) January–February and (b) June–July. Dotted-and-dashed lines show data [9] at altitudes of 15–25 km (T1) and 20–30 km (T2): (a) November–February and (b) May–August.

of E_p in the middle and high latitudes. Estimates of the impact of data-processing methods (vertical or horizontal detrending, type of filters, etc.) are given in [20, 25]. In particular, with vertical detrending (which was also used in our calculations) in the tropical zone, an additional contribution from planetary Kelvin waves falling within the filter range is possible. In the mid and high latitudes, vertical detrending can lead to underestimation of E_p due to the suppression of large-scale internal waves. Latitudinal distributions of E_p at heights of 20–25 km [20] show that vertical detrending in the tropics leads to an overestimation of E_p by up to 40%, and in the middle and high latitudes of the Southern Hemisphere in local summer–spring (May–October)—to an underestimation of up to 50%. Values of E_p obtained from the same experimental data, but with different filtration methods, can differ several times [25]. Thus, when analyzing the measurement data, in addition to the strong natural variability of IGW parameters, it is necessary to take into account the properties of the observational filter.

Figure 4 shows the latitudinal distribution of the integral potential energy averaged over two altitude intervals: 16–24 and 24–28 km. The results are shown for two seasons: January–February (left panel) and June–July (right panel). First, one should note the high E_p values in the equatorial zone, reaching 10–11 J/kg at altitudes of 16–24 km and 8–9 J/kg at heights of 24–28 km. The wave activity decreases rapidly with latitude, reaching E_p values of 3–4 J/kg in the middle latitudes and 1–2 J/kg at high latitudes. In these zones, the potential energy for heights of 24–28 km is slightly higher than in the lower range of heights (i.e., a flatter distribution at heights of 24–28 km). The latitudinal distribution of E_p does not show any obvious seasonal differences and, in general, this distribution is symmetric in both hemispheres. However, in the northern

latitudes above 60°, the winter E_p values are approximately twice as large as the summer ones.

It is interesting to compare our results with the data of the widely cited work [9], where, based on radio occultation measurements of the GPS/MET experiment in 1995–1997, the global distribution of potential energy was analyzed. In [9], in order to separate temperature fluctuations, filtration was performed in the scale interval 2–10 km. As follows from Fig. 4, our data generally agree with the data of [9], but there are still some differences. In [9], an increased activity of waves at high latitudes in the local winter is noted: in the Northern Hemisphere (left panel), this effect is small; in the Southern Hemisphere (right panel) in the 50° S–80° S band, it is quite noticeable. In addition, in [9], seasonal asymmetry is noted in the tropics at altitudes of 20–30 km: E_p in November to February is noticeably higher than in May to August.

In [17], the latitudinal distribution of monthly averaged E_p values at altitudes of 18–25 km in the Northern Hemisphere, obtained on the basis of a long-term archive of radiosonde data, is given. High IGW activity is noted in the tropical zone: $E_p = 4–9$ J/kg. However, the quadratic detrending used in [17] over the 18–25 km interval can lead to an underestimation of E_p at low latitudes due to the smoothing of fluctuations on scales close to the outer one (compare curves 4 in Fig. 1). In middle latitudes, E_p was 2–4 J/kg and, in the polar zone, it was 1–2 J/kg. Larger values of potential energy for high latitudes were observed mainly in winter. The high correlation between the potential energy and the dominant wavelength indicates the crucial role of the external scale in the wave energy in accordance with relations (1) and (2). The data of radiosonde measurements in Antarctica (69° S, 39.6° E) in 1997–1999 are presented in [39]. A filter with scales from 2 to 8 km was used to separate temperature fluctuations. At heights of 20–22 km, the E_p values were 0.5–2.0 J/kg,

the minimum values were observed in December to February (local summer), and the maximum values were observed in August to October (local spring). In [43], radiosonde data obtained in the tropics over northern Australia in October to December 2001 are presented. To separate temperature fluctuations, a filter with scales less than 3 km was used. The E_p values at altitudes of 20–30 km are 2–6 J/kg. These estimates seem to be significantly underestimated because large-scale fluctuations, especially significant in the tropics, are not taken into account.

The continuous monitoring of global IGW activity can only be provided by satellite, primarily radio occultation, measurements. We will carry out further comparative analysis using data from radio occultation temperature profiles. In [43], the radiosonde data are compared with the latitudinal distribution E_p in tropical latitudes from -30° to $+30^\circ$ derived from CHAMP data. At altitudes of 20–25 km, a sharp maximum is observed above the equator, reaching 10–12 J/kg, with a decrease to 2–4 J/kg towards the boundaries of this latitudinal interval. At altitudes of 25–30 km, $E_p = 3$ –5 J/kg and is distributed approximately evenly. However, as was indicated above, these estimates are most likely underestimated. In [31], the E_p distribution in the latitude band from -60° to $+60^\circ$ is given, obtained by filtering the profiles in the wavelength interval 2.5–10 km. In the tropics, E_p reaches 5–9 J/kg and, in middle latitudes, 2–5 J/kg, depending on the season. There was a local maximum at 60° S in June. In [22], on the basis of CHAMP data for 2001–2005, wave activity was studied in the polar regions (50° – 80° in both hemispheres). To separate temperature fluctuations, we used a filter at wavelengths of 2–7 km. At altitudes of 19–26 km for the Arctic, E_p values from 1.0 J/kg (in summer) to 3.0 J/kg (in winter) were obtained. In Antarctica, the E_p values varied from 1.0 J/kg in summer to 2.0 J/kg in winter, and the winter wave activity is less pronounced than in the Northern Hemisphere.

In [24], Fig. 9 shows the altitude–latitude distributions of E_p in different seasons of 2001–2003. To separate temperature fluctuations, a filter with an upper boundary of 10 km was used. In tropical latitudes from -30° to $+30^\circ$, E_p values decrease with altitude from 18 J/kg at 20 km to about 10 J/kg at 25 km, and further to 6 J/kg at 30 km. In middle latitudes, on the contrary, E_p increases from 2–3 J/kg at 20 km to 4–6 J/kg at 30 km. The E_p distribution in the lower and middle latitudes is weakly dependent on the season. The polar regions are characterized by significant seasonal asymmetry. In the Northern Hemisphere, maxima up to 4 J/kg correspond to winter, while in summer, minima of 1–2 J/kg were observed. In the Southern Hemisphere, maxima of up to 5–6 J/kg were observed in the spring, and the minima of 1–2 J/kg corresponded to summer. Latitudinal distributions of E_p in 2001–2008 were obtained in [40] based on CHAMP

data in a 5-km layer, the lower boundary of which was located 5 km above the tropopause. E_p maxima are noted in the tropics, reaching 10 J/kg. In the middle latitudes, E_p values were about 2 J/kg and, in the polar zones, 1–2 J/kg, with a weakly pronounced seasonal asymmetry. In [20], to distinguish fluctuations, vertical and horizontal methods of detrending were used. For vertical detrending, as in [9], a filter with a scale of 2–10 km was used, and Fig. 10 shows the latitudinal distribution of E_p in the 20–25 km altitude interval for May to October. The tropics correspond to a maximum of $E_p \approx 7$ J/kg and, at middle latitudes, 2–3 J/kg. At high latitudes, a significant latitudinal asymmetry is observed: in the Southern Hemisphere, E_p reaches 4 J/kg (increased winter–spring activity) and, in the Northern Hemisphere, E_p values are about 1 J/kg. In [44, 45], a method was developed for reconstructing high-resolution temperature profiles (about 200 m vertically) from satellite observations of the chromatic scintillations of stars. In [45], according to measurements of fast photometers GOMOS (Global Ozone Monitoring by Occultation of Stars), in 2002–2011, the latitudinal distribution of E_p was restored. Temperature fluctuations were allocated from individual profiles by a filter with an upper boundary of 4 km. There is a high activity of waves in the tropics (up to 5 J/kg), in the middle latitudes $E_p = 2$ –3 J/kg. There is also a strong seasonal dependence at high latitudes: in winter in the north, in the polar region, E_p values reached 3–4 J/kg and, in the Southern Hemisphere, the maximum E_p with values up to 5 J/kg was observed in winter–spring at a latitude of about 60° S.

Finally, we conclude that our estimates of E_p are generally consistent with the above data from radiosonde and GPS measurements, taking into account the natural variability of wave parameters and the influence of measurement methods and data processing. However, our data do not show the increased winter–spring wave activity noted in a number of studies in the high latitudes of the Southern Hemisphere. This may be partly due to the limited number of samples used, in addition to the strong variability in wave parameters.

CONCLUSIONS

This article presents the results of approbation of the previously developed technique for reconstructing the statistical parameters of internal waves in the stratosphere from fluctuations in the signal amplitude in a radio occultation experiment [1]. The method is based on the statistical description of a random ensemble of internal waves and the field of fluctuations of the radio signal amplitude generated by them. To solve the direct problem—calculating the statistical characteristics of amplitude fluctuations in a random environment—the parametric model of the three-dimensional IGW spectrum developed by A.S. Gurvich [2] was used, generalizing the one-dimensional

universal vertical spectrum of saturated internal waves [6–8]. In this technique, the external (characteristic) scale L_W and the structural characteristic C_W^2 are reconstructed. The outer scale defines the transition from unsaturated waves to saturated waves, and the structural characteristic is the only parameter that determines the spectral amplitude of saturated waves.

Approximations of the phase screen and weak fluctuations result in simple analytical relationships between the spectra of amplitude fluctuations of the radio signal and internal waves. The problem is solved taking into account the diffraction of radio waves; therefore, the resolution of the method is limited only by noise and is several hundred meters [11].

Previously, to study IGWs from radio occultation data, temperature profiles were used, which were reconstructed using the following approximations: (1) geometric optics and (2) local spherical symmetry [21, 27]. The first one limits the scales under study to the Fresnel zone, which is 1–1.5 km in the stratosphere. The second of these approximations leads to the smoothing of waves with horizontal scales less than 250–300 km [27, 31, 46].

Our method uses the assumption of local homogeneity of a random field of inhomogeneities in a spherical atmospheric layer, which imposes weaker conditions on the possible anisotropy of the investigated inhomogeneities [2]. The parametrization of the problem using a model spectrum of internal waves and a sufficiently high vertical resolution of the method make it possible to separately reconstruct the L_W and C_W^2 parameters of spectra in the scale range of interest, which increases the efficiency of modeling and parameterization of waves.

The choice of spectrum parameterization can introduce additional differences when compared with the data of other works. The method used is in many respects similar to the method of satellite eclipsing observations of star scintillations [3–5]. However, the difference in wavelengths by almost six orders of magnitude leads to significant differences in sensitivity to atmospheric disturbances, in the type and scale of irregularities, and in resolution [11]. The same differences allow the methods to complement each other both in the range of heights and in the investigated types and scales of inhomogeneities.

To test the method, we limited ourselves to the altitude–latitude distribution of the parameters of internal waves: external scale L_W , structural characteristic C_W^2 , temperature standard deviation $\sigma_{\delta T}$, and specific potential energy E_p . These distributions were calculated for heights of 16–24 and 24–28 km and for two seasons, January–February and June–July, based on the COSMIC 2011 measurements. Sources and estimates of possible errors associated with various measurement methods and data processing

methods are considered. The results are in satisfactory agreement with the data of radiosonde and GPS measurements of other authors, taking into account the possible differences and errors associated with the specific methods of measurements and processing, as well as the limited amount of processed data and high intermittency of IGWs.

A more detailed global distribution, taking into account the meridional dependence, is of great interest, since practically all works on the global distribution of wave activity indicate its significant meridional variability [9, 23, 24, 34, 45]. To restore the spatiotemporal distribution over the cells, 1 month–15 degrees of latitude–15 degrees of longitude, over 100 events in each cell (providing a 10% statistical error), an approximately 1-year archive of COSMIC measurement data is required.

The parameters of internal waves have a significant natural variability, as follows, for example, from long-term probe data obtained in the same place above a flat underlying surface and processed by the same, single method [18]. In individual measurements, the spectral amplitudes of temperature fluctuations differed by more than an order of magnitude, and the exponent of the spectrum in the saturation range varied from -2 to -4 . As also indicated in [18], the experimental data often differ from the model of the universal spectrum of saturated waves in the exponent, in the spectral amplitude in troposphere, and in the dependence on the Brunt–Väisälä frequency [6–8]. At the same time, the temperature spectra have a certain universality in relation to the time of day, season, and type of regular wind and temperature profiles.

In addition to natural variability, the results of IGW studies can differ significantly due to differences in measurement methods and data processing, which indicates the need for their unification [20, 25]. The strong spatiotemporal variability of IGW parameters, along with an understanding of the role of IGWs in the dynamics of the atmosphere, indicate the need to develop new methods for the global monitoring of waves. The comparison of our results with the data of other works shows that our method can be successfully used for monitoring IGWs in the middle atmosphere.

ACKNOWLEDGMENTS

V.F. Sofieva thanks the Academy of Finland (The Finnish Centre of Excellence in Inverse Problems and the TT-AVA project).

FUNDING

V. Kan, M. E. Gorbunov, and O. V. Fedorova are grateful for support from the Russian Foundation for Basic Research (grant no. 20-05-00189 A).

REFERENCES

1. Kan, V., Gorbunov, M.E., Shmakov, A.V., and Sofieva, V.F., "Reconstruction of the parameters of internal gravity waves in the atmosphere from amplitude fluctuations in a radio occultation experiment," *Izv., Atmos. Oceanic Phys.*, 2020, vol. 56, no. 5, pp. 435–437. <https://doi.org/10.1134/S0001433820050072>
2. Gurvich, A.S. and Brekhovskikh, V.L., "Study of the turbulence and inner waves in the stratosphere based on the observations of stellar scintillations from space: A model of scintillation spectra," *Waves Random Media* 2001, vol. 11, no. 3, pp. 163–181.
3. Gurvich, A.S. and Kan, V., "Structure of air density irregularities in the stratosphere from spacecraft observations of stellar scintillation. 1. Three-dimensional spectrum model 3D and recovery of its parameters," *Izv., Atmos. Oceanic Phys.*, 2003, vol. 39, no. 3, p. 300–310.
4. Gurvich, A.S. and Kan, V., "Structure of air density irregularities in the stratosphere from spacecraft observations of stellar scintillation. 2. Characteristic scales, structure characteristics, and kinetic energy dissipation," *Izv., Atmos. Oceanic Phys.*, 2003, vol. 39, no. 3, p. 311–321.
5. Sofieva, V.F., Gurvich, A.S., Dalaudier, F., and Kan, V., "Reconstruction of internal gravity waves and turbulence parameters in the stratosphere using GOMOS scintillation measurements," *J. Geophys. Res.*, 2007, vol. 112, p. D12113. <https://doi.org/10.1029/2006JD007483>
6. Dewan, E.M., and Good, R.F., "Saturation and the "universal" spectrum for vertical profiles of horizontal scalar winds in atmosphere," *J. Geophys. Res.*, 1986, vol. 91, no. D2, pp. 2742–2748. <https://doi.org/10.1029/JD091iD02p02742>
7. Smith, S.A., Fritts, D.C., and Van Zandt, T.E., "Evidence of saturation spectrum of atmospheric gravity waves," *J. Atmos. Sci.*, 1987, vol. 44, no. 10, pp. 1404–1410.
8. Fritts, D.C., "A review of gravity wave saturation processes, effects, and variability in the middle atmosphere," *Pure Appl. Geophys.*, 1989, vol. 130, no. 2/3, pp. 343–371.
9. Tsuda, T., Nishida, M., Rocken, C., and Ware, R.H., "A global morphology of gravity wave activity in the stratosphere revealed by the GPS occultation data (GPS/MET)," *J. Geophys. Res.*, 2000, vol. 105, no. D6, pp. 7257–7273.
10. Fritts, D.C. and Alexander, M.J., "Gravity wave dynamics and effects in the middle atmosphere," *Rev. Geophys.*, 2003, vol. 41, no. 1. <https://doi.org/10.1029/2001RG000106>
11. Kan, V., Gorbunov, M.E., and Sofieva, V.F., "Fluctuations of radio occultation signals in sounding the Earth's atmosphere," *Atmos. Meas. Tech.*, 2018, vol. 11, pp. 663–680. <https://doi.org/10.5194/amt-11-663-2018>
12. Sofieva, V.F., Gurvich, A.S., and Dalaudier, F., "Gravity wave spectra parameters in 2003 retrieved from stellar scintillation measurements by GOMOS," *Geophys. Res. Lett.*, 2009, vol. 36, pp. L05811. <https://doi.org/10.1029/2008GL036726>
13. Tsuda, T., Van Zandt, T.E., Mizumoto, M., Kato, S., and Fukao, S., "Spectral analysis of temperature and Brunt–Vaisala frequency fluctuations observed by radiosondes," *J. Geophys. Res.*, 1991, vol. 96, no. D9, pp. 17265–17278.
14. Gurvich, A.S., "Fluctuations in the observations of extraterrestrial cosmic sources through the Earth's atmosphere," *Radiophys. Quantum Electron.*, 1984, vol. 27, no. 8, pp. 665–672.
15. Kan, V., Sofieva, V.F., and Dalaudier, F., "Variable anisotropy of small-scale stratospheric irregularities retrieved from stellar scintillation measurements by GOMOS/Envisat," *Atmos. Meas. Tech.*, 2014, vol. 7, pp. 1861–1872. <https://doi.org/10.5194/amt-7-1861-2014>
16. Kan, V., "Stellar scintillations in spacecraft occultation experiment for atmospheric irregularities with variable anisotropy," *Atmos. Oceanic Opt.*, 2015, vol. 29, pp. 42–55. <https://doi.org/10.1134/S1024856016010085>
17. Wang, L., Geller, M.A., and Alexander, M.J., "Spatial and temporal variations of gravity wave parameters. Part I: Intrinsic frequency, wavelength, and vertical propagation direction," *J. Atmos. Sci.*, 2005, vol. 62, no. 1, pp. 125–142.
18. Nastrom, G.D., Van Zandt, T.E., and Warnock, J.M., "Vertical wavenumber spectra of wind and temperature from high-resolution balloon soundings over Illinois," *J. Geophys. Res.*, 1997, vol. 102, no. D6, pp. 6685–6701.
19. Wang, L., and Alexander, M.J., "Global estimates of gravity wave parameters from GPS radio occultation temperature data," *J. Geophys. Res.*, 2010, vol. 115, p. D21122. <https://doi.org/10.1029/2010JD013860>
20. Schmidt, T., Alexander, P., and de la Torre, A., "Stratospheric gravity wave momentum flux from radio occultations," *J. Geophys. Res.: Atmos.*, 2016, vol. 121, p. 4443–4467. <https://doi.org/10.1002/2015JD024135>
21. Steiner, A.K., and Kirchengast, G., "Gravity wave spectra from GPS/MET occultation observations," *J. Atmos. Ocean Technol.*, 2001, vol. 17, no. 4, pp. 495–503.
22. Hei, H., Tsuda, T., and Hirooka, T., "Characteristics of atmospheric gravity wave activity in the polar regions revealed by GPS radio occultation data with CHAMP," *J. Geophys. Res.*, 2008, vol. 113, p. D04107. <https://doi.org/10.1029/2007JD008938>
23. Rapp, M., Dörnbrackl, A., and Kaifler, B., "An intercomparison of stratospheric gravity wave potential energy densities from METOP GPS radio occultation measurements and ECMWF model data," *Atmos. Meas. Tech.*, 2018, vol. 11, pp. 1031–1048. <https://doi.org/10.5194/amt-11-1031-2018>
24. Ratnam, M.V., Tetzlaff, G., and Jacobi, C., "Global and seasonal variations of stratospheric gravity wave activity deduced from the CHAMP/GPS satellite," *J. Atmos. Sci.*, 2004, vol. 61, no. 13, pp. 1610–1620.
25. John, S.R. and Kumar, K.K., "A discussion on the methods of extracting gravity wave perturbations from space-based measurements," *Geophys. Res. Lett.*, 2013, vol. 40, pp. 2406–2410. <https://doi.org/10.1002/GRL.50451>

26. Alexander, M.J., "Interpretations of observed climatological patterns in stratospheric gravity wave variance," *J. Geophys. Res.*, 1998, vol. 103, no. D8, pp. 8627–8640.
27. Kursinski, E.R., Hajj, G.A., Schofield, J.T., Linfield, R.P., and Hardy, K.R., "Observing Earth's atmosphere with radio occultation measurements using the global positioning system," *J. Geophys. Res.*, 1997, vol. 102, no. D19, pp. 23429–23465.
28. Gorbunov, M.E. and Lauritsen, K.B., "Analysis of wave fields by Fourier Integral Operators and its application for radio occultations," *Radio Sci.*, 2004, vol. 39, no. 4, p. RS4010.
<https://doi.org/10.1029/2003RS002971>
29. Gorbunov, M.E., *Fizicheskie i matematicheskie printsipy sputnikovogo radiozattmennogo zondirovaniya atmosfery Zemli* (Physical and Mathematical Foundations of Satellite Radio Occultation Probing of the Earth's Atmosphere), Moscow: GEOS, 2019.
30. Murphy, D.J., Alexander, S.P., Klekociuk, A.R., Love, P.T., and Vincent, R.A., "Radiosonde observations of gravity waves in the lower stratosphere over Davis, Antarctica," *J. Geophys. Res.*, 2014, vol. 119, p. 996.
<https://doi.org/10.1002/2014JD022448>
31. Tsuda, T., and Hocke, K., "Vertical wave number spectrum of temperature fluctuations in the stratosphere using GPS occultation data," *J. Meteorol. Soc. Jpn.*, 2002, vol. 80, no. 4B, pp. 925–938.
32. de la Torre, A. Schmidt, T. and Wickert, J., "A global analysis of wave potential energy in the lower stratosphere derived from 5 years of GPS radio occultation data with CHAMP," *Geophys. Res. Lett.*, 2006, vol. 33, p. L24809.
<https://doi.org/10.1029/2006GL027696>
33. Hindley, N.P., Wright, C.J., Smith, N.D., and Mitchell, N.J., "The southern stratospheric gravity wave hot spot: individual waves and their momentum fluxes measured by COSMIC GPS-RO," *Atmos. Chem. Phys.*, 2015, vol. 15, pp. 7797–7818.
<https://doi.org/10.5194/acp-15-7797-2015>
34. Alexander, S.P., Tsuda, T., and Kawatani, Y., "Cosmic GPS Observations of Northern Hemisphere winter stratospheric gravity waves and comparisons with an atmospheric general circulation model," *Geophys. Res. Lett.*, 2008, vol. 35, p. L10808.
<https://doi.org/10.1029/2008GL033174>
35. McDonald, A.J., "Gravity wave occurrence statistics derived from paired COSMIC/FORMOSAT3 observations," *J. Geophys. Res.*, 2012, vol. 117, p. D15406.
<https://doi.org/10.1029/2011JD016715>
36. Chane-Ming, F., Molinaro, F., Leveau, J., Keckhut, P., and Hauchecorne, A., "Analysis of gravity waves in the tropical middle atmosphere over La Reunion Island (21° S, 55° E) with lidar using wavelet techniques," *Ann. Geophys.*, 2000, vol. 18, pp. 485–498.
37. Marquard, C. and Healy, S.B., "Measurement noise and stratospheric gravity wave characteristics obtained from GPS occultation data," *J. Meteorol. Soc. Jpn.*, 2005, vol. 83, no. 3, pp. 417–428.
38. Gubenko, V.N., Pavelyev, A.G., Salimzyanov, R.R., and Pavelyev, A.A., "Reconstruction of internal gravity wave parameters from radio occultation retrievals of vertical temperature profiles in the Earth's atmosphere," *Atmos. Meas. Tech.*, 2011, vol. 4, pp. 2153–2160.
<https://doi.org/10.5194/amt-4-2153-2011>
39. Yoshiki, M., "Energy enhancements of gravity waves in the Antarctic lower stratosphere associated with variations in the polar vortex and tropospheric disturbances," *J. Geophys. Res.*, 2004, vol. 109, p. D23104.
<https://doi.org/10.1029/2004JD004870>
40. Schmidt, T., de la Torre, A., and Wickert, J., "Global gravity wave activity in the tropopause region from CHAMP radio occultation data," *Geophys. Res. Lett.*, 2008, vol. 35, p. L16807.
<https://doi.org/10.1029/2008GL034986>
41. Alexander, S.P. and Tsuda, T., "Observations of the diurnal tide during seven intensive radiosonde campaigns in Australia and Indonesia," *J. Geophys. Res.: Atmos.* 2008, vol. 113, p. D04109.
<https://doi.org/10.1029/2007JD008717>
42. Sofieva, V.F., Dalaudier, F., Kivi, R., and Kyrö, E., "On the variability of temperature profiles in the stratosphere: implications for validation," *Geophys. Res. Lett.*, 2008, vol. 35, p. L23808.
<https://doi.org/10.1029/2008GL035539>
43. Tsuda, T., Ratnam, M.V., May, P.T., Alexander, M.J., Vincent, R.A., and MacKinnon, A., "Characteristics of gravity waves with short vertical wavelengths observed with radiosonde and GPS occultation during DAWEX (Darwin Area Wave Experiment)," *J. Geophys. Res.* 2004, vol. 109, p. D20S03.
<https://doi.org/10.1029/2004JD004946>
44. Dalaudier, F., Sofieva, V.F., Hauchecorne, A., Kyrölä, E., Blanot, L., Guirlet, M., Retscher, C., and Zehner, C., in *Proc. First Atmos. Sci. Conf. (Frascati, Italy, 8–12 May 2006)*.
45. Sofieva, V.F., Dalaudier, F., Hauchecorne, A., and Kan, V., "High-resolution temperature profiles retrieved from bichromatic stellar scintillation measurements by GOMOS/Envisat," *Atmos. Meas. Tech.*, 2019, vol. 12, pp. 585–598.
<https://doi.org/10.5194/amt-12-585-2019>
46. Belloul, M.B. and Hauchecorne, A., "Effect of periodic horizontal gradients on the retrieval of atmospheric profiles from occultation measurements," *Radio Sci.*, 1997, vol. 32, no. 2, pp. 469–478.

Translated by V. Selikhanovich